cells approached the overall performance achieved with n-type systems, although substantial photovoltages have been noted for strongly reducing solutions such as Eu(III)/Eu(II) in acid.[11]

In some cases, cell voltages have appeared insensitive to redox potentials and have thus been limited in value. This has led to the suggestion that p-type photocathodes made of covalently bound semiconductors, e.g., p-Si, p-GaAs, and p-InP, all exhibit pinning of the fermi level of the semiconductor surface and are subject to a "$^1/_3$ band-gap rule",[21] with the consequence that photovoltages ought not exceed $^1/_3$ of the band gap. Our results contradict these generalizations. We find that by judicious choice of the redox system and electrode pairing, a high-efficiency p-type photoelectrochemical cell is feasible.

The single-crystal p-InP photocathode used was grown by the gradient freeze method[29] and had Zn doping to $2.4 \times 10^{17}$ cm$^{-3}$, a mobility of 87 cm$^2$ V$^{-1}$ s$^{-1}$, and a bulk resistivity of 0.287 Ω cm. The crystal was sliced to yield (111) faces and then polished with an alumina slurry followed by lens paper impregnated with methanol-2% bromine. The A face of (111) InP, consisting entirely of In atms, was exposed to the solution.

A low-reflectance black surface finish was obtained by modifying the 1:6:6 HCl-$HNO_3$-$H_2O$ etch[30] to 1:2:2. An ohmic back-contact was produced by successively evaporating 300-Å Zn and 1000-Å Au and heating to 450 °C for 15 s. Details of electrode mounting have been reported previously.[10] The V(II)/V(III) redox couple solution contained 0.35 M total vanadium. The solution was prepared by reacting 3 N purity $V_2O_5$, a small excess of 6 N Zn over V(V) → V(II) stoichiometry, and sufficient electronic grade HCl to yield 4 M after the reduction. The solution potential was adjusted by access of air or additional Zn to −0.48 ± 0.02 V vs. SCE. At this potential, the solution shows three absorption maxima; 400 nm ($\epsilon$ 6.4 cm$^{-1}$ mol$^{-1}$, half-width, $\Delta$ = 100 nm), 600 nm ($\epsilon$ 4.5 cm$^{-1}$ mol$^{-1}$, $\Delta$ = 150 nm), and 890 nm ($\epsilon$ 0.8 cm$^{-1}$ mol$^{-1}$, $\Delta$ = 120 nm). Carbon counter-electrodes and magnetic stirring were used.

Stability tests under tungsten-halogen illumination of the p-InP/$VCl_3$-$VCl_2$-HCl/C cell showed stable maximum power point characteristics at 50 mA cm$^{-2}$ and 0.5 V in extended (3 days) operation. No measurable (±1 mg) weight change was observed upon passage of 13 000 C cm$^{-2}$. Furthermore, no deterioration in current, voltage, fill factor, or electrode weight was found upon cycling between short-circuit and open-circuit conditions while accumulating 3000 C cm$^{-2}$.

Figure 1 shows the current-voltage curve for a p-InP/$VCl_3$-$VCl_2$-HCl/C cell illuminated by natural sunlight of an incident irradiance of 110 mW/cm$^2$. The short-circuit current density is 25 mA cm$^{-2}$, the open-circuit voltage 0.66 V, and the fill factor 0.63. The maximum solar-to-electrical power conversion efficiency is thus 9.4%. The difference between the experimentally observed short-circuit current density and the 39 mA cm$^{-2}$ theoretically predicted[31] for the above irradiance at the band gap of InP (1.35 eV at room temperature) can be accounted for by solution absorbance and reflection losses.

We propose that the exceptional stability and performance of the new cell are due to the fast kinetics of the V(II)/V(III) couple, the suitable placement of the band edges, our nonreflective surface finish, and the unique surface chemistry of InP. The latter is probably the most important factor. It is known that the surface recombination velocity of vacuum-cleaved n-InP decreases upon oxidation by exposure to air from $10^6$ cm s$^{-1}$ to $10^3$ cm s$^{-1}$.[32,33] Futhermore, the exceptionally high solar power conversion efficiency of indium oxide and indium tin oxide junctions of InP compared to corresponding junctions of other III-V compounds has been clearly related to the interfacial chemistry.[34] The formation of a very thin oxide layer on the surface of the p-InP electrode is likely upon either exposure to air or reaction with water. The observations on the oxidation of InP and the resultant reduction in the surface recombination velocity have been interpreted in a previous paper[35] as being due to the saturation of reactive surface bonds by oxygen. Such saturation reduces the density of interface states in those semiconductors that are oxidized exclusively to stable oxides with large energy gaps. In view of the large free energy of formation of both indium and phosphorus oxides and of their large band gaps, it is expected that some of the states characteristic of oxidized InP interfaces will be above and below the band edges and thus will not limit the performance of solar cells. For this reason, one would predict well-behaved liquid junctions independent of whether a bulk oxide film seals the InP surface or whether chemisorbed oxygen accounts for the removal of interface states.[35] Note that for GaAs, the thermodynamic instability of the arsenic oxide/GaAs system[36-38] may lead to the formation of free arsenic and gallium oxide at the interface. Arsenic will introduce states between the edges of the valence and conduction bands. It may be responsible for the high recombination velocity and, in some cases, for pinning of the fermi level at the surface of GaAs. As a consequence of this basic difference in the surface chemistry of GaAs and InP, no noticeable reduction is observed in the $10^6$ cm s$^{-1}$ free-surface recombination rate after exposure of GaAs to air.[32,39-41] A confirmation of the expectation based on this interpretation is that p-InP photocathode based liquid junction cells exhibit power conversion efficiencies substantially superior to cells with p-GaAs photocathodes.[11,19-21]

**Acknowledgment.** We thank S. Menezes for useful discussions and experimental assistance, F. A. Thiel for the growth of the p-InP crystal, its processing, and contacting, and R. G. Vadimsky for assistance with the solar measurements.

**Note Added in Proof**: Addition of $RuCl_3 \cdot 3H_2O$ or insertion of a Pt wire cause rapid evolution of hydrogen by the reaction

$$V^{2+} + H^+ \rightarrow V^{3+} + {}^1/_2H_2$$

This suggests the feasibility of photoassisted electrolysis in the cell

$$\text{p-InP}/V^{3+} - H^+(\text{catalyst})\ H^+/\text{Pt}$$

(27) VanWezemael, A. M.; Laflère, W. H.; Cardon, F.; Gomes, W. P. *J. Electroanal. Chem. Interfacial Electrochem.* **1978**, *87*, 105.
(28) Vervaet, A. A. K.; Gomes, W. P.; Cardon, F. *J. Electroanal. Chem. Interfacial Electrochem.* **1978**, *91*, 133.
(29) Bachmann, K. J.; Buehler, E. *J. Electron. Mater.* **1974**, *3*, 279.
(30) Thiel, F. A.; Barns, R. L. *J. Electrochem. Soc.* **1979**, *126*, 1272.
(31) Hovel, H. J. "Semiconductors and Semimetals, Solar Cells", Academic Press: New York, 1975; Vol. II, p 38.
(32) Casey, H. C., Jr.; Buehler, E. *Appl. Phys. Lett.* **1977**, *30*, 247.
(33) Suzuki, T.; Ogawa, M. *Appl. Phys. Lett.* **1979**, *34*, 447.
(34) Bachmann, K. J.; Schreiber, H.; Sinclair, W. R.; Schmidt, P. H.; Thiel, F. A.; Spencer, E. G.; Pasteur, G.; Feldman, W. L.; SreeHarsha, K. *J. Appl. Phys.* **1979**, *50*, 3441.
(35) Heller, A. In "Chemical Control of Surface and Grain Boundary Recombination in Semiconductors" in "Photoeffects at Semiconductor-Electrolyte Interfaces", Nozik, A. J., Ed.; American Chemical Society: Washington, D.C., 1980.
(36) Thurmond, C. D.; Schwartz, G. P.; Kamlott, G. W.; Schwartz, B. *J. Electrochem. Soc.* **1980**, *127*, 1366.
(37) Schwartz, G. P.; Griffiths, J. E.; DiStefano, D.; Gualteri, G. J.; Schwartz, B. *Appl. Phys. Lett.* **1979**, *34*, 742.
(38) Watanabe, K.; Hashiba, M.; Hirohata, Y.; Nishino, M.; Yamashina, T. *Thin Solid Films* **1979**, *56*, 63.
(39) Jastrzebski, L.; Lagowski, J.; Gatos, H. C. *Appl. Phys. Lett.* **1975**, *27*, 537.
(40) Jastrzebski, L.; Gatos, H. C.; Lagowski, J. *J. Appl. Phys.* **1977**, *48*, 1730.
(41) Hoffman, C. A.; Jarasiunas, K.; Gerritsen, H. J.; Nurmikko, A. V. *Appl. Phys. Lett.* **1978**, *33*, 536.

**A. Heller,* B. Miller, H. J. Lewerenz, K. J. Bachmann**
*Bell Laboratories*
*Murray Hill, New Jersey 07974*
*Received June 9, 1980*

## Theoretical Study of a Low-Energy UV Transition in a 2,6-Dithiaadamantane Derivative

*Sir:*

Recently, we have reported that bis($\gamma$,$\gamma$-dimethylallenyl) sulfone (**1**) undergoes a novel and facile base-catalyzed cyclodimerization to the 2,6-dithiaadamantane derivative 4,8,9,10-tetraisopropylidene-2,6-dithiaadamantane tetraoxide (**2**).[1] Surprisingly,

(1) Braverman, S.; Reisman, D.; Sprecher, M.; Rabinovich, D.; Frolow, F. *Tetrahedron Lett.* **1979**, *10*, 901.

0002-7863/80/1502-6556$01.00/0 

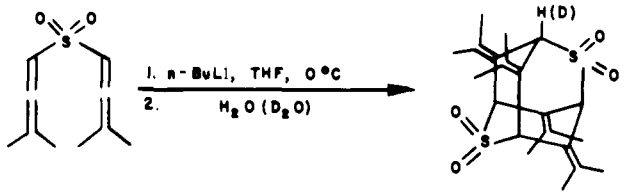


1 2

it was also found that compound **2** shows a strong ultraviolet absorption at $\lambda_{max}$ = 236 nm with $\epsilon \sim 29\,000$ in acetonitrile and $\sim 24\,500$ in 95% ethanol. Such $\epsilon$ values in solution are typical of allowed electronic transitions, and the $\lambda_{max}$ value indicates an unusually low-energy electronic excitation, considering that the olefinic double bonds in 2 are not conjugated. Typical $\lambda_{max}$ values for the first allowed transition in nonconjugated polyolefins are ~200 nm. These electronic transitions must be of non-Rydberg character because of their high intensity in a condensed phase where Rydberg-type bands are typically "washed out" because of their diffuse nature.

A preliminary analysis of possible electronic interactions in **2** indicated that both through-space and through-bond interactions between the nonconjugated double bonds must be invoked to properly account for this transition and its intensity. Through-space and through-bond interactions have been studied[2-5] with regard to their effect on the orbital ionization energy ordering. However, not much attention has been paid to the effect of these interactions on the excited electronic states of the neutral compound. On the basis of symmetry considerations and molecular orbital calculations, it will be shown here that the low-energy UV band in **2** is the result of a transition to an excited-state orbital (the LUMO) which is stabilized by through-space interactions. On the other hand, through-bond interactions acting on the energy ordering of the highest occupied orbital energy levels cause the low-energy transition to be symmetry allowed and therefore strong in intensity.

The dithiaadamantane **2** belongs to the $D_{2d}$ symmetry group.[6] The main $S_4$ axis passes through both sulfur atoms, and the planes of the two sulfonyl ($SO_2$) groups are at orthogonal angles to each other. The perpendicular $C_2'$ axes each pass through a pair of double bonds along the olefinic carbon–carbon axis. Thus, the four olefinic carbon–carbon axes lie in a plane with all the olefinic methylene groups at a fixed angle (45°) to this plane (see Figure 1).

Because the $SO_2$ groups are not expected to make any significant contribution to the electronic transition energy[7] in the region of the 236-nm absorption observed for **2**, the interactions of the noncoplanar olefinic bonds were investigated to elucidate the nature of the electronic transition responsible for this absorption. The system of four nonconjugated double bonds was studied by using ab initio self-consistent field methods, first as four separate ethylene molecules by using the symmetry and interatomic distances found in **2**, and second in the whole molecule 1,3,5,7-tetramethylenecyclooctane (**3**), preserving the carbon skeletal frame structure of **2**. All calculations were carried out

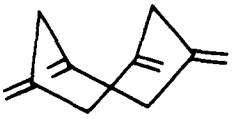

**3**

in the well-known STO-3G basis[8] with the GAUSSIAN-70 program.

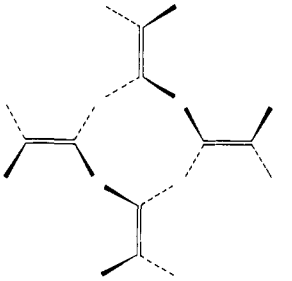

**Figure 1.** Geometry of the four olefinic double bonds. The carbon–carbon $\sigma$ bonds are in the paper's plane, and the methylene groups are at 45° to this plane.

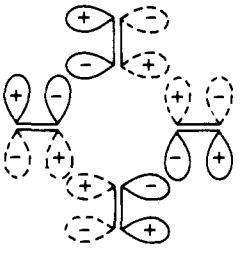

a.

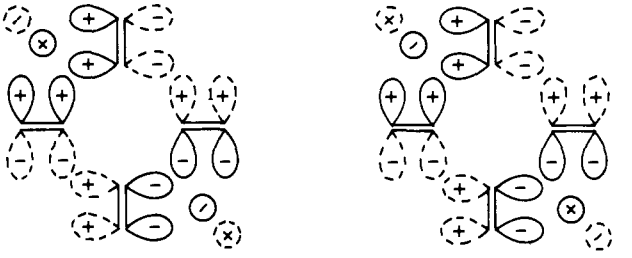

b.

**Figure 2.** (a) $\phi_{b_2}$ ($\pi^*$) orbital. The four carbon–carbon $\sigma$ bonds are in the paper's plane, and the orbital lobes are at 45° to this plane. (b) $\phi_e$ ($\pi$) orbital interaction with the methylene groups (this orbital is one of the doubly degenerate). On the left is the bonding combination; on the right is the antibonding combination.

**Table I.** ab Initio STO-3G Energies and Symmetries of Highest Occupied and Lowest Unoccupied Molecular Orbitals

| molecular orbitals | orbital energy, au |
|---|---|
| four ethylene units | |
| $\phi_{b_2}$ ($\pi^*$) | 0.2908 |
| $\phi_{a_2}$ ($\pi$) | −0.2868 |
| $\phi_e$ ($\pi$) | −0.3136 |
| $\phi_{b_2}$ ($\pi$) | −0.3497 |
| tetramethylenecyclooctane | |
| $\phi_{b_2}$ ($\pi^*$) | 0.2557 |
| $\phi_e$ ($\pi$) | −0.2614 |
| $\phi_{a_2}$ ($\pi$) | −0.2954 |
| $\phi_{b_2}$ ($\pi$) | −0.3233 |
| $\phi_e$ | −0.4055 |

As a check on the adequacy of this level of approximation, a dimer consisting of only two adjacent ethylene units as found in **2** was calculated in the 4-31G basis, and the results ($\pi$ and $\pi^*$ energy splittings) were found to be very similar to the STO-3G basis results.[9] In addition, the molecular orbitals of the full dithiaa-

(2) Hoffmann, R.; Heilbronner, E.; Gleiter, R. *J. Am. Chem. Soc.* **1970**, *92*, 706.
(3) Hoffmann, R. *Acc. Chem. Res.* **1971**, *4*, 1.
(4) Heilbronner, E.; Martin, H. D. *Helv. Chim. Acta* **1972**, *55*, 1490.
(5) Goldstein, M. J.; Natowsky, S.; Heilbronner, E.; Hornung, V. *Helv. Chim. Acta* **1973**, *56*, 294.
(6) The X-ray crystal structure analysis has been done, and the results will be published elsewhere.
(7) Jaffe, H. H.; Orchin, M. "Theory and Application of Ultraviolet Spectroscopy"; Wiley: New York, 1962; p 481.
(8) Hehre, W. J.; Lathan, W. A.; Ditchfield, R.; Newton, M. D.; Pople, J. A. *QCPE* **1973**, *11*, 236.
(9) The total energy of two noninteracting ethylene units is lower than the total energy of two interacting ethylenes because of the antiaromatic character of the $\pi$ electronic system.
(10) Howell, J.; Rossi, A.; Wallace, D.; Haraki, K.; Hoffmann, R. *QCPE* **1978**, *11*, 344.

damantane (**2**) were calculated by the extended Hückel method,[10] and the symmetries and energy ordering of the highest occupied levels matched the ab initio results obtained for 1,3,5,7-tetramethylenecyclooctane (**3**).

Table I summarizes the ab initio results for the HOMOs and the LUMO. The orbital energy splittings of the four occupied olefinic $\pi$ bonds due to through-space interactions in the first model (four ethylene units) are 0.06 au (1.6 eV). The magnitude of this energy splitting indicates[11] that the perturbing effect of one ethylenic $\pi$ system on the other is significant. The lowest unoccupied molecular orbital is $\phi_{b_2}$ ($\pi^*$). The outstanding feature of this orbital is that besides the internal $\pi^*$ antibonding nature of each olefin unit, a given carbon atom $p_\pi$ atomic orbital overlaps (bonding) two different neighboring $p_\pi$ atomic orbitals on adjacent double bonds, thus creating double-concentric overlapping systems of the inner-ring and outer-ring $p_\pi$ orbitals (Figure 2a). Consequently, the energy of the $\pi \rightarrow \pi^*$ excited state in which this group $\pi^*$ orbital is occupied is expected to be lowered, leading to a long-wavelength electronic transition in the olefinic chromophore.

Still, the picture is incomplete because the predicted lowest energy transition from Table I, $a_2 \rightarrow b_2$ ($B_1$), is symmetry forbidden in the $D_{2d}$ point group. In order to study the possible through-bond interactions, four methylene groups were placed at a single carbon–carbon bond distance between adjacent ethylene units to create the 1,3,5,7-tetramethylenecyclooctane **3**. The four $>CH_2$ units form group orbitals made up of the C–$H_2$ $\sigma$ orbitals, all of which belong to the $a_1$, $b_2$, and e symmetry representations in $D_{2d}$. The new group orbitals of e symmetry interact with the $\phi_e$ ($\pi$) orbital (Figure 2b), and this interaction is sufficient to cause a splitting in the $\phi_e$ ($\pi$) energy level so that it becomes the highest occupied molecular orbital (see Table I). The lowest unoccupied molecular orbital is still the $\phi_{b_2}$ ($\pi^*$) discussed before, and the HOMO $\rightarrow$ LUMO transition, $e \rightarrow b_2$, is now symmetry allowed.

Recently, Paquette[12,13] et al. studied structures like hexaquinacene, which also constitute a cyclic arrangement of nonconjugated double bonds. Analogous to what was found here, an inversion of the energy ordering of highest occupied levels was also observed, apparently due to an interaction between the olefinic $\pi$ system with the $\sigma$ frame. However, a cyclic overlapping $p_\pi$ orbital system cannot be formed in this case because of the odd number of olefinic double bonds. Therefore, as observed, the UV spectrum of hexaquinacene shows the normal olefinic double-bond wavelength absorption (192 nm).

**Acknowledgment.** We thank Professor M. Sprecher for his critical reading of the manuscript.

(11) Hemmersbach, P.; Klessinger, M. K.; Bruckman, P. *J. Am. Chem. Soc.* **1978**, *100*, 6344.
(12) Paquette, L. A.; Wallis, T. G.; Kempe, T.; Christoph, G. G.; Springer, J. P.; Clardy, J. *J. Am. Chem. Soc.* **1977**, *99*, 6946.
(13) Christoph, G. G.; Muthard, J. L.; Paquette, L. A.; Böhm, M. C.; Gleiter, R. *J. Am. Chem. Soc.* **1978**, *100*, 7789.

**Samuel Braverman, Drora Cohen,* David Reisman Harold Basch**
*Department of Chemistry*
*Bar-Ilan University, Ramat-Gan, Israel*
*Received January 9, 1980*

## Chelation of the Sodium Cation by Polyamines: A Novel Approach to Preferential Solvation, and to the Understanding of Sodium-23 Chemical Shifts and Quadrupolar Coupling Constants

*Sir:*

Important technological processes such as electrolysis, and liquid–liquid extraction, depend critically upon the influence of dissolved salts on phase equilibria.[1-3] Much effort is applied to obtain a better understanding of the preferential solvation of ions in solvent mixtures.[4,5] NMR methods are especially well-suited for such investigations.[5-10] We report here the marked changes undergone by the $^{23}$Na chemical shifts for $NaClO_4$ with the composition of binary solvent mixtures of THF with amines.[11] These changes are analyzed in a novel application of the Hill formalism.[12] With unidentate amines (pyridine, piperidine, pyrrolidine, aniline, propylamine, and isopropylamine), there is equality of the intrinsic equilibrium constants $k$ for the successive steps upon displacement of THF from sodium coordination by one of these ligands.[13] The results, which are entirely consistent with tetracoordination of the sodium cation by these solvents,[13] also indicate proportionality of the $k$ values to the amine chemical shifts. With bidentate amines (ethylenediamine, diethylenetriamine, 1,3-diaminopropane, and cadaverin), entries of the first and second diamine molecules into the sodium coordination shell are independent and equiprobable steps:[14,15] $k_1 = k_3$ and $k_2 = k_4$. This also affords a direct intramolecular measurement of the chelate effect[14] from the molar ratio of the two solvates $\alpha_2/\alpha_1$ (Scheme I). The apparent equilibrium constants $K_i$ are related to the *intrinsic* equilibrium constants $k_i$ ($i$ = 1–4) through the statistical factors appearing in Scheme I.

Scheme I

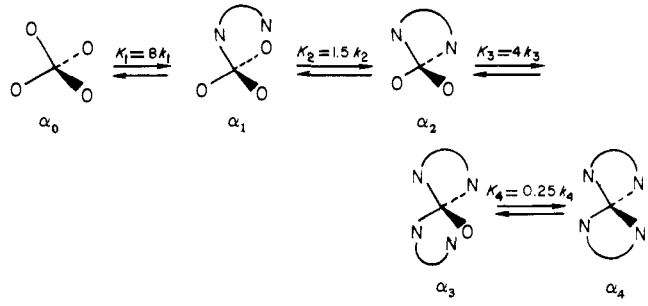


Table I. Values of the Intrinsic Equilibrium Constants ($k$) for the Successive Replacement of THF Molecules by Amine Solvents[a]

| solvent | $k_1$ | $k_1k_2$ | $k_3$ | $k_3k_4$ |
|---|---|---|---|---|
| cdv | 0.9 | 20 | 1.1 | 43 |
| dap | 0.4 | 38 | 0.5 | 35 |
| eda | 1.5 | 110 | 1.1 | 95 |

[a] Cadaverin (cdv), 1,3-diaminopropane (dap), and ethylenediamine (eda).

A Hill plot is a representation of ln ($Y$/1 – $Y$) as a function

(1) Furter, W. F. *Can. J. Chem. Eng.* **1977**, *55*, 229–239.
(2) de Visser, C.; Perron, G.; Desnoyers, J. E.; Heuvelsland, W. H.; Somsen, G. *J. Chem. Eng. Data* **1977**, *22*, 74–79.
(3) Parker, A. J. *Electrochim. Acta* **1976**, *21*, 671–679.
(4) Langford, C. H.; Tong, J. P. K. *Pure Appl. Chem.* **1977**, *49*, 93–97.
(5) Covington, A. K.; Newman, K. E. *Adv. Chem. Ser.* **1976**, No. *155*, 153–196; *Pure Appl. Chem.* **1979**, *57*, 2041–2058.
(6) Detellier, C.; Laszlo, P. *Helv. Chim. Acta* **1976**, *59*, 1333–1345; *Ibid.* **1976**, *59*, 1346–1351.
(7) Detellier, C.; Gerstmans, A.; Laszlo, P. *Inorg. Nucl. Chem. Lett.* **1979**, *15*, 93–97.
(8) Holz, M.; Weingärtner, H.; Hertz, H. G. *J. Chem. Soc., Faraday Trans. 1* **1977**, *73*, 71–83.
(9) Holz, M.; Weingärtner, H.; Hertz, H. G. *J. Solution Chem.* **1978**, *7*, 705–720.
(10) Briggs, R. W.; Hinton, J. F. *J. Solution Chem.* **1979**, *8*, 519–527.
(11) $^{23}$Na NMR spectra were recorded on a Bruker W.P. 80 instrument at 21.16 MHz, with an external $C_6D_6$ lock (8.5 μs, 90° pulse length, spectral window of 6024 Hz, 8K data points, S/N > 60:1 in THF-rich solutions, S/N > 20:1 in amine-rich solutions).
(12) Hill, A. V. *J. Physiol. (London)* **1910**, *40*, iv–xi.
(13) Delville, A.; Detellier, C.; Gerstmans, A.; Laszlo, P. *Anal. Chem.*, submitted for publications.
(14) Delville, A.; Detellier, C.; Gerstmans, A.; Laszlo, P. *Anal. Chem.*, submitted for publication.
(15) The $k$ values were derived from simultaneous optimization, using the Simplex procedure,[16] of the calculated changes in chemical shifts and in line widths (corrected for the viscosity) with composition of the binary solvent mixture. The full procedure is described in another article.[14]
(16) Deming, S. N.; Morgan, S. S. *Anal. Chem.* **1973**, *45*, 278A–282A.

0002-7863/80/1502-6558$01.00/0 